Trends in Peptide and Protein Sciences
Volume 6 (2021): e6

DOI: http://dx.doi.org/10.22037/tpps.v6i0.36423

Original Article

Preparation, Optimization and *in vitro* Studies of Spectrin Decorated Liposomes: A Promising Strategy for Cancer Treatment

Tanweer Haider, Sandeep Dubey, Indu Lata Kanwar, Vikas Pandey and Vandana Soni*

[a] *Department of Pharmaceutical Sciences, Dr. Harisingh Gour University, Sagar, Madhya Pradesh, India-470003.*

Article history:
Received: 14 October 2021
Accepted: 13 November 2021

Keywords:
Design of Experiment
Liposomes
Phosphatidylserine
Phosphatidylethanolamine
Spectrin
Tumor membrane targeting

HIGHLIGHTS

- Optimization of liposomes using Design of Experiment.
- Drug sustained released from liposomes and followed a non-Fickian diffusion anomalous transport.
- Spectrin-liposomes target the exposed membrane phospholipids of cancer cells.
- Spectrin decorated liposomes showed 50% of maximal inhibition of cell proliferation in U373-MG cells more significant plain liposomes.

ABSTRACT

The distorted membrane asymmetry and abnormal distribution of phospholipids viz. phosphatidylserine (PS) and phosphatidylethanolamine (PE), in the outer leaflet are one of the critical features of cancer. It is a much-known fact that protein, such as spectrin (SPC), has an affinity towards the PS and PE. Hence, SPC was used to target exposed PS and PE of cancer cells. In the present study, the drug Methotrexate was used because it disrupts and fluidized the plasma membrane. Liposomes prepared and optimized by the Response Surface Box Behnken randomized model using various independent and dependent variables. The optimized liposomes were further coated with SPC and the coating confirmed by infrared spectroscopy. Both formulations were further characterized for vesicle size, entrapment efficiency (EE), zeta potential, surface morphology, and percentage of drug released. The results indicate that the prepared formulations were in spherical, nano-metric size with negative zeta potential and more than 75% drug entrapment with sustained release pattern. The concentration for 50% of maximal inhibition of cell proliferation (GI50) in U373-MG cells was found to be 24.11±0.44 and 3.90±0.19 µg/mL of the formulations MTX-LP2 and SPC-MTX-LP2, respectively. Briefly, results suggest that the developed liposomes could be used for enhanced cancer treatment.

Cite this article as: Haider, T., Dubey, S., Kanwar, I. L., Pandey, V. and V. Soni, (2021). Preparation, optimization and *in vitro* studies of spectrin decorated liposomes: A promising strategy for cancer treatment. *Trends Pept. Protein Sci.*, **6**: e6.

Introduction

Cancer is a life-threatening disease which results due to undisciplined growth of healthy cells, causing malignancy. As per the World Health Organization

T. Haider: https://orcid.org/0000-0002-7391-815X
V. Soni: https://orcid.org/0000-0002-4118-0779

*Corresponding Author:
Email: vsoni@dhsgsu.edu.in; drvandanasoni@gmail.com (V. Soni)

(WHO) report, cancer is the world's second most leading death-causing disease and responsible for approximately ten million deaths in 2018 (Wang et al., 2011; WHO, 2021). Lack of early detection and proper and effective treatment are crucial factors of death due to cancer. Healthy cells and tissues are very well organized through the production and release of growth-promoting signal, which affects the cell cycle, including healthy cell growth and apoptosis. On the other hand, cancer cells possess their own different capabilities like specific signals for proliferation, bypassing growth suppressors, resisting cell death, immortality, angiogenesis followed by invasion and metastasis for their survival (Gutschner and Diederichs, 2012). Cancer cells can adopt some alternative mechanisms by which cells prevent apoptosis and enhance nutrient uptake and angiogenesis for proliferation (Jin et al., 2007). The morphological and physiochemical changes in cancer cells as compared to healthy cells are other distinct characteristics that include bilayer membrane's integrity where the plasma membrane phospholipids' asymmetry gets altered. The loss of asymmetric distribution of various phospholipids from their sole position is one of the cancerous cells' pathological conditions and biomarkers (Winter et al., 2015; Sharma and Kanwar, 2018).

The plasma membrane of normal healthy cells possesses an asymmetric distribution of phospholipids in the membrane leaflets (Quinn, 2004; Elvas et al., 2017), i.e., the PS and PE localized in the cell's inner membrane leaflet; whereas, phosphatidylcholine (PC) and sphingomyelin (SG) in outer leaflets (Spector and Yorek, 1985; Zwaal and Schroit, 1997; Winter et al., 2015). On another side, the plasma membrane of cancer cells has abnormal symmetry, i.e., PS and PE are exposed on the outer leaflet of the cells (Sugimura et al., 1994; Neves et al., 2013; Haider et al., 2019), which may be due to oxidative stress (Fadok et al., 1992; Emoto et al., 1997). This changed physiological condition could be a useful tool to target the antitumor drug against cancer. Hence, in the present study, we try to develop a delivery system with a specific affinity towards the "changed physiology," i.e., exposed PS and PE at the outer leaflet of the cancer plasma membrane.

SPC is a protein and chief constituent of the cell membrane and red blood cells (RBCs) skeleton (Machnicka et al., 2012). Various studies have been suggested that SPC has an affinity towards neutral phospholipids (Grzybek et al., 2006; Ray and Chakrabarti, 2004; Pathak and Mallik, 2017), such as PE and PC and negatively charged PS (Mombers et al., 1980; Sikorski et al., 2000), thus could be used as ligand for various drug targeting at tumor sites.

MTX is a commonly used chemotherapeutic agent, immunosuppressant, and competitive inhibitor of dihydrofolate reductase. But due to some systemic toxicity (Gottschalk et al., 2015; Alves et al., 2016) and development of drug resistance (Alekseeva et al., 2017), the effectiveness of the MTX is reduced. MTX encapsulation in a nano-vesicular delivery system may be a promising means to improve its pharmacological properties and protect the drug from the non-targeted interaction with circulatory biomolecules. It has been reported that MTX has interaction with the polar head of membrane phospholipids and fluidized the lipoidal center of bilayers. As a result, the pores' formation occurs, leading to the disarrangement packing of lipids and finally disrupting membrane integrity (Maheswari, 2001). Further, SPC's conjugation with MTX-bearing liposomes makes it an unerring system by binding with exposed PE and PS to kill cancer cells. The proposed engineered carrier system also protects from the other side effects of MTX to healthy cells due to targeted carriers' specificity. Liposomes are nanosized, sphere-shaped vesicles containing one or more phospholipid bilayers composed of cholesterol and natural nontoxic phospholipids. These are emerging technologies for rational delivery as they provide improved pharmacokinetic properties, controlled and sustained release of drugs, and more importantly, low systemic toxicity and ability to trap both lipophilic and hydrophilic drugs (Malam et al., 2009; Akbarzadeh et al., 2013). Liposome properties vary greatly with lipid composition, surface charge, size and method of preparation. Drug encapsulated liposomal systems have been found to have the ability to protect the stability and integrity of therapeutic molecules and to deliver the therapeutic agent to the desired target sites (Soni et al., 2007; Tiwari et al., 2020). Several investigations have shown that liposomes can localize to tumor cells, which are known for their high endocytic activity, and can become a convenient vehicle for drugs used in cancer chemotherapy (Soni et al., 2008; Lakkadwala et al., 2019; Lujan et al., 2019). In this regard, SPC, decorated MTX-loaded liposomes constitute a promising drug delivery system for the transport of cytotoxic drugs to the tumor site.

In this study, we prepared and evaluated the plain MTX-loaded liposomes and SPC-decorated MTX-loaded liposomes for targeted and efficacious treatment of the tumor. Distearoyl-sn-glycerol-3-phosphoethanolamine (DSPE) was used to formulate liposomes, which helps in the coating of SPC over the surface of liposomal vesicles. The SPC guided delivery of liposomes represents an efficient strategy to design an efficient formulation, which means it provides a maximum

accumulation of drugs at the target site and avoids drug interaction with healthy cells (Dubey et al., 2004; Patel et al., 2016). SPC decorated liposomes may have driven force to bind with PS and PE present on the target site, i.e., the plasma membrane of cancer cells, and facilitates MTX delivery. The MTX bearing liposomes decorated with SPC was developed for effective cancer treatment with minimal side effects for neighbouring healthy cells. The proposed study will be a promising strategy for cancer therapy.

Materials and Methods

Chemicals

MTX was procured as a gift sample from M/s Bimal Pharma Private Limited, Mumbai, India. DSPE was procured as a gift sample from Lipoid GmbH, Germany. Cholesterol (CHOL), soya Phosphatidylcholine (PC), chloroform, and methanol were purchased from CDH, India. Spectrin from human erythrocytes purchased from Sigma-Aldrich (USA). Phosphate buffer, phenylmethanesulfonyl fluoride, Triton X-100, Sephadex G-50, Sephadex G-200, trichloroacetic acid (TCA), dimethyl sulfoxide (DMSO) and sodium chloride were purchased from HiMedia Laboratory Pvt. Ltd., Mumbai, India. All other chemicals used were of analytical reagent grade.

Response surface Box Behnken randomize design

The response surface methodology is a set of mathematical and statistical techniques based on fitting a polynomial equation to a set of experimental data in order to make statistical predictions (Myers et al., 2016) RSM has been used in studies involving the investigation of complex multi-variable systems and analyze the interaction of independent variables (factors) and their impact on the dependent variables (responses) (Haider et al., 2020; García-Beleño and Rodríguez de San Miguel, 2021).

Box-Behnken designs (BBDs) are response surface designs that are specifically designed to require only three levels, denoted as -1, 0 and +1. BBDs are available for three to twenty-one factors. They are developed by combining two-level factorial and incomplete block designs. BBD creates designs with desirable statistical properties while also requiring a fraction of the experiments required for a three-level factorial. BDDs contain three levels for each factor and are specifically designed to fit a quadratic model. The BBD lacks runs at the most extreme combinations of all the factors, but compensates by having superior prediction precision in the center of the factor space. While a run or two may be erroneous in these designs, the accuracy of the observations in the remaining runs is important to the model's dependability. Although categorical elements can be added to these designs, the design is repeated for each categorical treatment combination (Ferreira et al., 2007; Ejikeme et al., 2013; Robinson, 2014). Randomized BBD, is a response surface design of BBD, have the capacity to vary all factor levels between runs. This is done to prevent against a lurking variable effect, as well as to guarantee that each run is exposed to the same sources of variation from factor level setting.

Preparation and optimization of MTX-liposomes

Liposomes were prepared by using cast film method, as reported by Bangham with some modifications (Bangham, 1968). Briefly, different molar ratio of PC: CHOl: DSPE (7: 1: 1, 6: 1: 1, and 5: 1: 1) and methotrexate (5, 10 and 15 mg) were taken as per the formulation design (Table 1). The amount of DSPE was kept constant in all the formulations. The lipids and MTX were dissolved in a mixture of chloroform: methanol in a ratio of 2: 1 (10 mL). The flask containing this mixture was attached to the rotatory evaporator (Super Fit, Ambala, India), and solvent was allowed to evaporate resulting in the formation of thin transparent film. After a thin film was formed, the flask was kept overnight for complete removal of solvent. After 24 h, the film was hydrated with 10 mL of PBS (pH 6.4) and rotated in the opposite direction for 1 h. The resultant liposomes were sonicated for a different period (2, 4 and 6 min) using a probe sonicator (Sonics Vibra cell®) to form smaller vesicles.

Further, prepared formulations were lyophilized (Vertis wizard 2.0®) at -80^{o}C and 100 mTorr for 24 h and stored at 4^{o} C. The formulations were optimization by Design of Experiment (DoE) using response surface Box Behnken randomized quadratic design with no blocks and DoE were constructed with the help of design expert-10 (Stat-Ease Inc., MN, and Version 10.0.1.0) software. Three independent variables/factors, i.e., amount of MTX (A), PC molar ratio (B), and sonication time (C) with three levels (+1, 0, and -1, which represents as high, medium, and low levels) were used to establish their impact on dependent variables/responses, i.e., vesicles size (R1) and EE (R2) and find the three-dimension (3D) surface response (Table 2). All other processes and formulation parameters were kept constant during optimization. Different factors and responses were taken in the formulation design are summarised in Table 1.

Table 1. Different formulations and their factors and responses for the optimization of formulations. Data are represented in mean ±SD and n= 3

Run	Formulations	Factors			Responses*	
		Amount of MTX (mg)	Soya PC molar ratio	Sonication time (min)	Mean vesicle size (nm)	Entrapment efficiency (%)
1	MTX-LP1	15	6	6	367.3±1.42	58.81±2.34
2	MTX-LP2	10	6	4	172.7±3.25	81.04±0.88
3	MTX-LP3	10	7	2	245.4±0.73	66.60±1.37
4	MTX-LP4	5	7	4	321.5±2.16	62.04±1.48
5	MTX-LP5	10	6	4	158.4±4.09	70.80±3.65
6	MTX-LP6	15	5	4	411.5±3.11	66.70±0.25
7	MTX-LP7	5	6	2	389.5±1.48	45.04±4.35
8	MTX-LP8	10	5	2	295.5±7.21	78.08±0.27
9	MTX-LP9	15	7	4	337.1±3.44	60.80±2.25
10	MTX-LP10	5	6	6	278.4±0.27	63.04±5.76
11	MTX-LP11	10	6	4	174.4±4.11	78.40±0.47
12	MTX-LP12	10	7	6	198.2±2.67	68.70±3.17
13	MTX-LP13	10	6	4	178.5±6.89	74.05±1.06
14	MTX-LP14	10	5	6	159.4±4.58	71.04±7.34
15	MTX-LP15	10	6	4	189.6±5.16	76.74±6.11
16	MTX-LP16	5	5	4	356.3±0.77	51.16±0.55
17	MTX-LP17	15	6	2	439.1±6.45	67.15±3.15

Table 2. Constrains for optimization and predicted solutions

Variables	Goal	Minimum limit	Maximum limit	Importance
A: Amount of MTX (mg)	In range	5	15	***
B: Soya PC molar ratio	In range	5	7	***
C: Sonication time (min.)	In range	2	6	***
R1: Vesicles size (nm)	Minimum	158.4	439.1	#
R2: Entrapment efficiency (%)	Maximum	45.04	81.04	#

A: Amount of MTX (mg)	B: Soya PC molar ratio	C: Sonication time (min.)	R1: Vesicles size (nm)	R2: Entrapment efficiency (%)	Desirability
9.814	6.079	6.079	159.493	75.754	0.922

*** Most significant and independent variables.
# Dependent variables.
Italics indicate the optimum run (formulation).

Determination of vesicles size

Firstly, 2 mg of all prepared liposomes (MTX-LP1-17) were diluted with deionized water and dispersed adequately. The vesicle size of drug-loaded liposomes formulations was determined by dynamic light scattering method using zeta sizer (Malvern Instruments Ltd., and Nanoplus particulate system). All the measurements were made at room temperature.

Determination of entrapment efficiency (EE)

The EE was determined after separation of the non-entrapped drug using the Sephadex G50 minicolumn centrifugation method (Fry et al., 1979). For column's preparation, about 1 g of Sephadex G50 was used and swollen in distilled water at room temperature with occasional shaking for at least 5 h, then stored at 4°C till further use. For minicolumns preparation, Whatman GF: B filter pads were inserted at the bottom of the barrels of 2.5 cm^3 syringes and filled with pre-swelling gel. Excess water was centrifuged off at 3000 rpm for 3 min using a lab centrifuge. The unentrapped drug from liposomes (MTX-LP1 to MTX-LP17) suspension was removed by passing the formulation through a Sephadex G-50 minicolumn and centrifuged at 3000 rpm for 2 min. The LPs were then lysed using 0.1% v/v Triton-X 100, and drug content was determined by using high performance

liquid chromatography by the Eq. 1. HPLC (Agilent 1100 series) was used with the photodiode array (PDA) detector. Synergy Polar-RP C18 columns (4 m, 75 mm x 2.0 mm) were chosen, and the column temperature was maintained at 40 °C. The mobile phase, which had a flow rate of 0.6 mL/min, as a mixture of acetonitrile (70%), 10 mM ammonium formate (15%), and 0.5 % formic acid (15%) was used. The wavelength of UV detection was set to 311 nm.

$$\%\ \text{drug entrapment}\ \frac{\text{Amount of drug entrapped in LPs}}{\text{Total amount of drug taken}} \times 100 \quad \text{(Eq.1)}$$

Based on minimum vesicle size and maximum EE, the formulation MTX-LP2 was found to be optimized. The optimized formulation, MTX-LP2, was selected for the preparation of SPC decorated liposomal formulation.

Preparation of SPC decorated liposome formulations

The optimized formulation was used for the SPC coating. The SPC decorated liposomes (SPC-MTX-LP2) was prepared by the cast film method as discussed in the section "preparation of MTX-liposomes". The hydration of film was done with 10µL of buffered aqueous glycerol solution of SPC and 10 mL of PBS (pH 6.4). The resultant SPC-MTX-LP2 were sonicated for an optimized time using probe sonicator to form smaller vesicles and then, lyophilized and stored at 4° C. The coating efficiency of SPC conjugated with MTX-2 was determined using the Folin-Ciocalteu reagent (Jain et al., 2016). The amount of uncoated SPC in the supernatant after washing was determined using a UV-visible spectrophotometer (Shimadzu® 1800, Japan) set to 750 nm. Eq. 2 was used to compute the percentage of conjugation.

$$\text{Percentage coating of SPC on liposomes} = \frac{\text{Initial added SPC} - \text{recovered SPC}}{\text{Initial added SPC}} \times 100 \quad \text{. (Eq. 2)}$$

Characterization of liposomal formulations

a) etermination of vesicles size, polydispersity index (PDI), zeta potential, and EE

The vesicle size of SPC-MTX-LP2 was determined using the procedure mentioned above in the "optimization of MTX-liposomes" section. The PDI and zeta potential of formulations MTX-LP2 and SPC-MTX-LP2 were determined by dynamic light scattering method using zeta sizer (Malvern Instruments Ltd., and Nanoplus particulate system). All the measurements were made at 25°C. The EE of SPC-MTX-LP2 was determined as mentioned in the above "optimization of MTX-liposomes" section.

b) Shape and surface morphology

The morphology of selected optimized formulations, i.e., MTX-LP2 and SPC-MTX-LP2, was studied by transmission electron microscope (TEM). The above samples were fixed with 2% phosphotungstic acid and examined under a TEM (FEI Tecnai TF20 IIT, New Delhi).

c) Infrared spectroscopy

Infrared spectroscopy of drug, excipient, drug-excipient mixture, MTX-LP2, and SPC-MTX-LP2 was performed by Fourier-transform infrared spectroscopy (FTIR) (PerkinElmer Spectrum, Version 10.03.06). The dried samples of excipients, a physical mixture of drug and excipients, MTX-LP2, and SPC-MTX-LP2, were placed separately on the sample holder. The spectra were scanned over 4000 to 400 cm^{-1}.

In vitro drug release study and data analysis

The formulations, i.e., MTX-LP2 and SPC-MTX-LP2, were centrifuged to remove the unentrapped drug. Then, 1mL of the pure liposomal suspension and 10 mg of pure MTX (control) were placed in a dialysis tube (VISKING dialysis tubing; MWCO12-14kD) and then placed in a beaker containing 20 mL of phosphate buffer saline (PBS) pH 6.8, separately. The solution containing the dialysis tube was stirred on a magnetic stirrer at a constant temperature of 37±0.5°C throughout the study. Samples (2 mL) were withdrawn at a derived time interval (0.5, 1.0, 1.5, 2.0, 2.5, 3.0, 4.0, 5.0, 6.0, 7.0, 8.0, 24 and 48 h.), passed through Whatman filter paper (#41) and analysed drug released by HPLC. The 2 mL of fresh PBS (pH 6.8) added after each withdrawal. The cumulative percentage of drug released was determined.

The five-drug release kinetic models, i.e., zero-order, first-order, Higuchi, Hixson-Crowell, and Korsmeyer-Peppas release equation were used to determine the release pattern and applied to interpret the release data. The values of R^2 for the above-stated drug release models were calculated.

In vitro cell proliferation

In vitro cell proliferation of MTX-LP2 and SPC-MTX-LP2 were evaluated by the SRB assay (Skehan et al., 1990; Vichai and Kirtikara, 2006) using human

glioblastoma astrocytoma U373-MG cells. The cell proliferation study was performed as per the method reported by Skehan *et al*. (Skehan et al., 1990). Briefly, U373-MG cells were cultured in RPMI 1640 medium having 10% fetal bovine serum and 2mM glutamic acid and inoculated in 96 microplates in100 µL at plating densities of 10,000 cells per well and incubated at 37° C with 5% CO_2 and 95% relative humidity for 24 h before adding experimental samples. The samples were diluted to get final drug concentrations such as 10, 20, 40, and 80 µg/mL with PBS (pH 6.8). The assay was terminated after 48 h by addition cold TCA. The cells were fixed for 1 h, at 4°C. The samples were washed five times, and 50 µl 0.4 % (w/v) SRB solution was added in each well and incubated for 20 min at room temperature. One percent (v/v) acetic acid was used to remove the unbound dye, and plates were dried, and then analyzed at a wavelength of 540 nm with 690 nm reference wavelength by using the plate reader. Adriamycin (ADR) was used in the same concentration range as a positive control. Cytotoxicity was expressed as the percentage of viable cells relative to incubated cells in the presence of 0.1% DMSO vehicle control. The percentage of growth inhibition (GI50) was calculated by Eq. 3. GI50 was calculated from the drug concentration, resulting in a 50% reduction in purified protein. Each measurement was done in triplicate.

$$\text{Percentage of growth inhibition} = \frac{\text{Ti}-\text{Tz}}{\text{C}-\text{Tz}} \times 100 \quad \text{(Eq.3)}$$

Where absorbance at zero time (Tz), control growth (C), and test growth of formulation in the presence of drug at four concentration levels (Ti)).

Statistical analysis

Microsoft® Excel and GraphPad Prism 8.01 were used to calculate mean and standard (SD) and data analysis. All samples were analyzed in triplicate to calculate SD, and data are presented as mean ± SD. Significance was compared with experimental groups using one-way analysis of variance (ANOVA) with the Turkish post hoc test. A value of $p < 0.05$ was considered statistically significant.

Results and Discussion

The plasma membrane of normal cells possesses the asymmetric distribution of phospholipids, but the asymmetric structure has been distorted in cancerous cells (Haider et al., 2019). PS and PE of cancer membrane phospholipids are significantly distributed on the outer membrane (Sugimura et al., 1994). SPC has interaction with these phospholipids (Mombers et al., 1980). In the present study, SPC has developed surface-modified liposomal drug carriers for more efficacious cancer treatment.

Preparation and optimization of MTX-liposomes

First, the plain dug loaded formulations were designed by the response surface Box Behnken experimental design and seventeen sets of LPs were prepared by modified cast film methods using soya PC, CHOL, DSPE in a different molar ratio in a mixture of 10 mL chloroform: methanol (2:1) and MTX as drug and then, optimized using response surface Box Behnken randomized model using different factors (amount of MTX, soya PC molar ratio and sonication time), and responses (vesicles size and EE). The 3D response surface plots obtained by using Design Expert Software were shown in Fig. 1. The optimum formulation parameters were selected based on a specified goal, i.e., vesicle size and percent EE. The highest polynomial showing the lowest p-value (<0.05) along with the highest Lack of Fit p-value (>0.1) was considered for model selection. For response one (R1), i.e., vesicle size, the p values for the linear, 2FI, quadratic, and cubic were found to be 0.5059, 0.9727, < 0.0001, and 0.0858, respectively. Similarly, p values for response two (R2), i.e., EE, were found to be 0.7211, 0.5208, 0.0014, and 0.3326 for linear, 2FI, quadratic, and cubic models, respectively. Whereas the lack of fit values for response vesicles size for the linear, 2FI, and quadratic were obtained as 0.0002, < 0.0001, and 0.0858, respectively, and for response EE, lack of fit values for response EE for the linear, 2FI, and quadratic were found be 0.0232, 0.0178 and 0.3326, respectively. The summary of ANOVA for responses vesicles size and EE were found to be "predicted R-squared" of 0.8074 and 0.1665 is in reasonable agreement with the "adjacent R-squared" of 0.9656 and 0.7956, i.e., <0.2. The "adequate precision" is 18.7176 and 8.5858, respectively, indicating an adequate signal for the model to be used to navigate the design space. Response surface quadratic model equation of design matrix with intercept (β_0) and the model co-efficient (β_1- β_9) to explore the possibilities of significant interactions between the responses (Y) and factors (A, B, and C) is shown in as Eq. 4.

$$Y = \beta_0 + \beta_1 A + \beta_2 B + \beta_3 C + \beta_4 AB + \beta_5 AC + \beta_6 BC + \beta_7 A^2 + \beta_8 B^2 + \beta_9 C^2 \quad \text{(Eq. 4)}$$

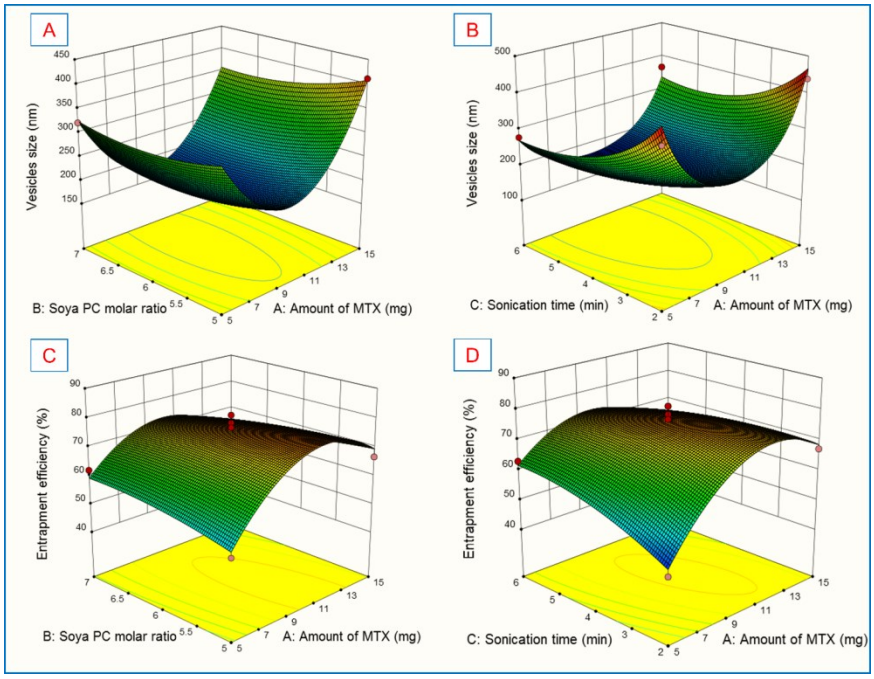

Figure 1. 3D surface response curves, the effect of soya PC molar ratio, amount of drug and sonication time on vesicles size (A & B), and entrapment efficiency (C & D).

The equation over the design matrix in terms of coded factors for prediction of responses R1 and R2 for a given level of each factor are mentioned below in Eq. 5 and Eq. 6:

$$\text{Vesicle size (R1)} = 177 + 26.16 * A - 15.06 * B - 45.78 * C - 9.90 * AB + 9.83 * AC + 22.22 * BC + 161.7 * A^2 + 17 * B^2 + 29.77 * C^2 \quad \text{(Eq. 5)}$$

$$EE(R2) = 76.21 + 4.02 * A - 1.10 * B + 0.5900 * C - 4.20 * AB - 6.59 * AC + 2.29 * BC - 14.31 * A^2 - 1.72 * B^2 + 3.38 * C^2 \quad \text{(Eq. 6)}$$

By default, the high levels of the factors are coded as +1, and the low levels are coded as -1; and the whole equation helps to identify the relative impact of the factors by comparing the factor coefficient.

The selection constraints and its desirability were found to be 0.922. The optimum formulation was selected with minimum vesicle size and maximum EE Y1= (158.4 ≤Y≤439.1) and Y2= (45.05≤Y≤81.04) (Table 2).

Two responses, such as mean vesicle size and EE, were used as optimization parameters. The vesicle size distribution of formulations MTX-LP1 to MTX-LP17 was found in the range between the 172.4± 3.25 to 411.5± 3.11 nm (Table 1). The percentage of entrapped drug was found in the range of 45.04±4.35% to 81.04±0.88%.

Using multiple linear regression analysis, different polynomial equations were evaluated to best fit the experimental data by determining the coefficients' values in the polynomial equations, and one full and reduced model was established. The 3D surface plots were useful in establishing the main effects (effect of individual variables) on the response parameter and insight into the combined effects of two variables. Validation of the employed experimental design and chosen model to its prediction capability for optimizing the variables was done by performing the check-point analysis. Statistical comparison between the predicted values and the average of three experimental values of the response parameters was performed to derive the percentage error and evaluate the significant difference between them. Out of the seventeen formulations, formulation MTX-LP2 was showed the minimum vesicle size and maximum EE. Hence, it was used as an optimized formulation, based on the criteria such as p values, lack of fit, etc., the quadratic model was best fitted to the observed responses. The summary of ANOVA for responses vesicles size and EE predicted R-squared was found in reasonable agreement with the adjacent R-squared. The adequate precision is indicating an adequate signal for the model to be used to navigate the design space.

The optimization was based on the desirability criteria that make the best trade-off between the constraints and selecting a combination that satisfies the

best criteria for the optimization and weighs the prediction based on a desirability index 0 (for the least suitable combination) to 1. The optimal concentration was searched throughout the experimental domain where the desirability function "r" closest to 1. Based on the maximum desirability, MTX-LP2 was found to best fit. In Fig. 1A & 1B, the 3D response surface, shed-like the curve of response mean vesicle size nonlinear increase with the increasing amount of drug. The 3D response surface (Fig. 1B) shows that vesicle size slightly decreased with the time of sonication time increased. It may due to the increased sonication time changes large multilamellar vesicle into the small bilayer vesicles (Korgel et al., 1998; Woodbury et al., 2006). In Fig. 1A, the 3D response surface shows that increasing soya PC/CHOL molar ratio slight decrease in vesicles size. The soya PC/CHOL molar increases decreased the molar concentration of CHOL in liposomes. CHOL provides stability and rigidity of the phospholipids layer. The reduced amount of CHOL may slightly increase the bilayer of phospholipids and increased swollen membrane structure (Manojlovic et al., 2008). Similarly, the amount of drug has nonlinear increased the drug entrapment (Fig. 1C). It may vary due to the drug available maximum in the vesicle of liposomes. The EE slightly increased with the increase soya PC: CHOL molar ratio (Fig. 1C), may due to the MTX solubility in the organic phase, which has a high affinity toward the phospholipids. The similar result showed in research (Ong et al., 2016), where EE of Griseofulvin increased with an increase of PC concentration. In Fig. 1D, with the increase of sonication time, EE nonlinearly increases. The increase sonication time produced the small and unilamellar vesicles. Silva *et al.* (2010) showed that the decrease of the particle size with the increase of the sonication time, until a plateau size obtained. Sonication is a commonly used method to create small, unilamellar vesicles from a lamellar dispersion and is well known to disrupt bilayer membranes. Sonication is a well-known way for creating small, unilamellar vesicles from a lamellar dispersion, and it is also well recognised for rupturing the bilayer membrane. The unilaminar and smaller sized vesicles contributed to more drug entrapment (Sou, 2011).

Decoration of optimized liposomes with SPC

Optimized MTX-LP2 was further used to develop the SPC decorated liposomes decorated (SPC-MTX-LP2) and characterized the different parameters. The percentage drug coating on the liposomes was found to be 11.3±0.74%. The coating of SPC on surface due to interaction between the lipid DSPE present in liposomes.

Characterization of liposome formulations

a) Vesicle size, PDI, zeta potential, and EE determination

The characterization of prepared formulations MTX-LP2 and SPC-MTX-LP2 were done by PDI and zeta potential, while SPC-MTX-LP2 was also characterized by mean vesicle size and EE. The vesicular size (Fig. 2) and EE of SPC-MTX-LP2 were found to be 245.4± 3.36 nm and 77.16± 5.2%, respectively (Table 3). PDI of MTX-LP2 and SPC-MTX-LP2 were found to 0.45± 0.013 and0.267± 0.009, respectively, and zeta potential (Fig. 2) of MTX-LP2 and SPC-MTX-LP2 were found to be -3.6± 0.68 and -27.8± 0.42 mV, respectively (Table 3). The mean vesicular size of SPC-MTX-LP2 was found to be slightly more significant than the MTX-LP2. The greater vesicular size may be due to the coating of SPC on the LPs surface (Haider et al., 2020). EE of SPC-MTX-LP2 was slightly lower than MTX-LP2. It may be due to the drug's leaching during coating with SPC (Pandey et al., 2018). The PDI is less than 0.5 showed the uniform and homogenous vesicles distribution. The zeta potential of the SPC-MTX-LP2 formulation was negative (-27.8± 0.42 mV) due to the net charge of the lipid and protein composition in the formulation. Zeta potential, representing the surface charge, indicates the stability of the formulation (Mozafari, 2010; Sou, 2011). Usually, a zeta potential value of -30 mV to +30 mV is considered sufficient repulsive force to achieve better physical stability (Joseph and Singhvi, 2019). This low value of the surface charge show good implicit stability by preventing coalescence of vesicles due to strong electrostatic repulsion interaction and helps in unilaminar vesicles formation. The zeta potential value of LPs was a negative which assist in adhesion to cancer cells and internalization by cellular endocytosis (Zhang et al., 2008).

b) Shape and surface morphology

The TEM photograph (Fig. 3) showed that MTX-LP2 and SPC-MTX-LP2 formulations were almost spherical in shape and also confirms their size range within the nano-limits. The TEM photographs of MTX-LP2 and SPC-MTX-LP2 were almost spherical in shape and nanometric in size. Because these structures are nanosized, they can penetrate the tissue system, allowing the drug to be easily uptake by cells, allowing for efficient drug delivery, and ensuring action at the desired location (Patra et al., 2018).

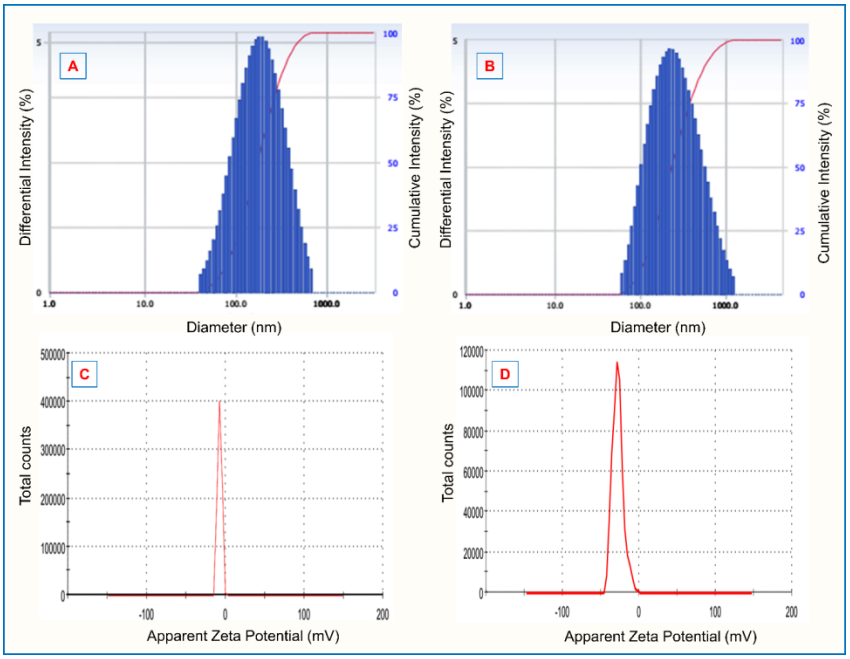

Figure 2. The vesicles size distribution of (A) MTX-LP2 and (B) SPC-MTX-LP2; zeta potential of (C) MTX-LP2 and (D) SPC-MTX-LP2.

Table 3. The means vesicle size, PDI Zeta potential, and %EE of MTX-LP2 and SPC-MTX-LP2 (n=3, ±SD)

Formulations	Mean vesicle size (nm)	PDI	Zeta potential (mV)	EE (%)
MTX-LP2	172.7± 3.25	0.45± 0.013	-3.6± 0.68	81.04± 0.88
SPC-MTX-LP2	245.4± 3.36	0.267± 0.009	-27.8± 0.42	77.16± 5.2

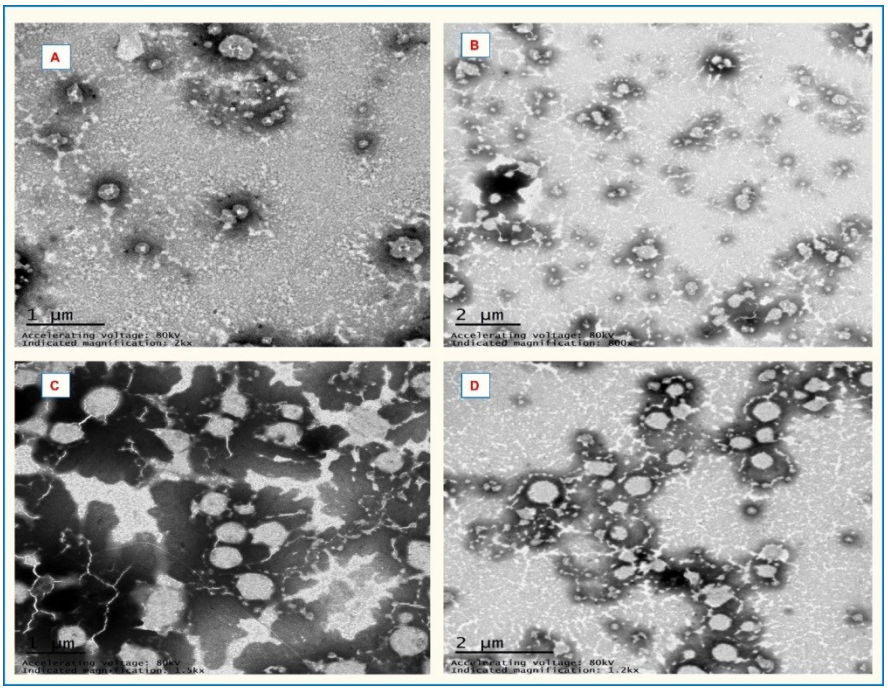

Figure 3. The TEM images (A) MTX-LP2 (2000X), (B). MTX-LP2 (800X) (C) SPC-MTX-LP2 (1500X), and (D) SPC-MTX-LP2 (1200X).

c) Infrared spectroscopy

The infrared spectroscopy was used for the confirmation of SPC coating over the liposomal surface and to study the drug-excipients compatibility study The obtained FTIR spectra (Fig. 4) of soya PC showed various peaks viz. 3362.92 cm^{-1} (-OH group, stretch, H bounded), 3010.14 cm^{-1} (=C-H stretch), 2955.29 cm^{-1}, 2924.34 cm^{-1} and 2853.59 cm^{-1} (-CH stretch), 1739.21 cm^{-1} (C=O stretch), 1646.26 cm^{-1} (C=C stretch), 1464.81 cm^{-1}(C=C stretch), and 1237.16 cm^{-1} (C-O-stretch). The characteristics IR peaks of CHOL was obtained, i.e., 3583.88 cm^{-1} and3382.66 cm^{-1} (-OH group, stretch, H bounded), 2930.57 cm^{-1} and 2866.62 cm^{-1} (-CH stretch), 1692 cm^{-1} (C=O stretch), (1649.67 cm^{-1} (C=C stretch), 1464.83 cm^{-1} (C=C stretch), 1375.91 cm^{-1},1055.74 cm^{-1} and 1021.99 cm^{-1} (C–O stretch of ester), and 762.12 cm^{-1} and 666.79 cm^{-1} (due to aromatic substitutions). The obtained FTIR spectra of DSPE having major peaks, i.e., 2954.52 cm^{-1}, 2917.45 cm^{-1} and 2849.13 cm^{-1}, (-CH stretch), 1741.47 cm^{-1} (C=O stretch), 1652.69 cm^{-1} (C=O stretch, amide), 1558.58 cm^{-1} (-NH bending), 1418.91 cm^{-1} and 1471.65 cm^{-1} (C=C stretch),1222.80 cm^{-1} (C-O-stretch) and 1080.12 cm^{-1} (C-O- stretch), and 950.15 cm^{-1} and 728.83 cm^{-1} (aromatic substitutions). FTIR spectrum of MTX showed the characteristic peaks such as 3464.82 cm^{-1} (-NH stretch), 1683.4 cm^{-1} (-COOH), 1645.79 cm^{-1} (-CONH), 853.588 cm^{-1} (aromatic stretch out- of- plane bend). The characteristic peaks of the MTX confirming the purity of the drug. The mixture of soya PC, CHOL, DSPE and MTX are 3354.70 cm^{-1} (-OH group, stretch, H bounded), 3009.83 cm^{-1} (=C-H stretch), 2925.51 cm^{-1} and 2853.15 cm^{-1} (-CH stretch), 1742.52 cm^{-1} (C=O stretch), 1651.90 cm^{-1} (C=O stretch, amide),1466.33 cm^{-1} (C=C stretch), 1378.14 cm^{-1}, 1055.31 cm^{-1}, and 1023.00 cm^{-1}, and 722.06 cm^{-1} (aromatic substitutions). The FTIR spectra of the mixture sample showed the compatibility between the drug and excipients. FTIR spectra of the formulation MTX-LP2, the major peaks of drugs were observed and merged at wavenumbers 3362.92 cm^{-1} (-OH group, stretch, H bounded), 3010.14 cm^{-1},2955.29 cm^{-1} and 2924.34 cm^{-1} (C-H stretch), 1739.21 cm^{-1} (C=O stretch), 1646.26cm^{-1} (N-H binding),1510.69 cm^{-1}, 1417.73 cm^{-1} and 1464. 05 cm^{-1} (C=C stretch), 1378.05 cm^{-1}, 1237.16 cm^{-1}, 1182.41 $cm^{-1}$and 1069.46 cm^{-1}(C-N amine), and 853.58 cm^{-1} and 667.68 cm^{-1} (aromatic substitutions). In the FTIR spectra of the formulation SPC-MTX-LP2, the major peaks of drugs were observed and merged at wavenumbers 3382.19 cm^{-1}, 2994.52 cm^{-1}, 2923.68 cm^{-1} and 2852.77 cm^{-1} (-CH stretch), 1739.12 cm^{-1}, 1652.75 cm^{-1}(C=C stretch), 1598.39 cm^{-1}, 1553.77 cm^{-1} and 1417.73 cm^{-1} (C=C stretch), 1378. 05 cm^{-1}, 1237.16 cm^{-1}, 1182.41 cm^{-1} and 1063.46 cm^{-1} (C-N amine), and 829.43 cm^{-1}, 770.12 cm^{-1} and 721.75 cm^{-1} for aromatic substitutions (Fig. 4**)**. The IR spectra confirmed that there was no interaction among excipients, and between drug and excipients was found. There were no abnormal peaks observed in the IR spectra of MTX-LP2 and SPC-MTX-LP2. The IR spectra also suggested that SPC coating on the surface was taken place without any chemical interactions. The two peaks, 1598.39 cm^{-1} and 1553.77 cm^{-1} characteristic peaks of Ca^{2+} binding protein SPC presence in SPC-MTX-LP2 (Nara et al., 1994; Mizuguchi et al., 1997).

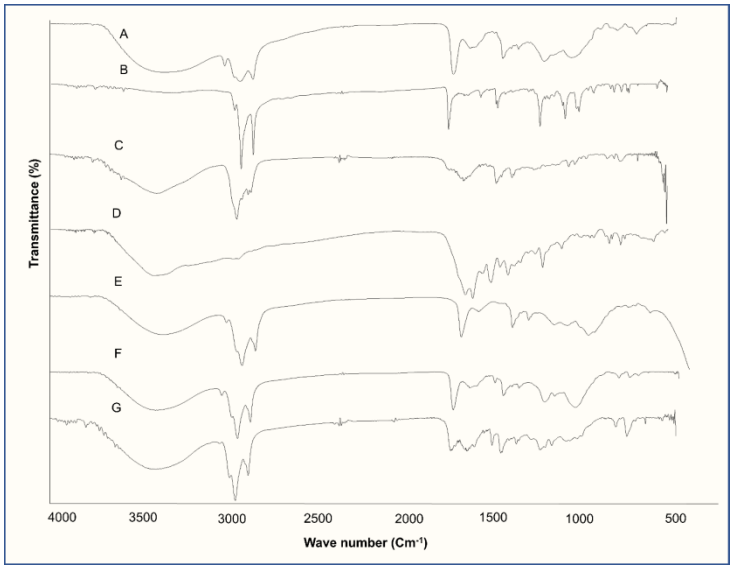

Figure 4. FTIR spectra. (A) soya PC, (B) CHOL, (C) DSPE, (D) MTX, (E) mixture of soya PC, CHOL, DSPE and MTX, (F) MTX-LP2, and (G) SPC-MTX-LP2.

In-vitro drug release study and data analysis

In-vitro drug release study of different liposomal formulations, i.e., MTX-LP2 and SPC-MTX-LP2, were performed in PBS (pH 6.8). The cumulative percentage of drug released from the different formulations was in the order of MTX-LP2 > SPC-MTX-LP2. The cumulative percentage drug release from the optimized formulation MTX-LP2 and SPC-MTX-LP2 was found to be 71.24±1.66% and 65.23±1.49%, respectively, after the 48 h of the study (Fig. 5). The release of the drug from the formulations were slow and sustained after 48 h of studies. At 48 h. the study, the drug released from SPC-MTX-LP2 was significantly ($p<0.001$) slower than MTX-LP2. It may due to the coating of SPC on the surface offer double barriers on the drug released from the formulations. The similar results were reported in previously developed formulations i.e., lectin conjugated nanoparticulate (Jain et al., 2016), and SPC conjugated nanoparticulate carrier system (Haider et al., 2020). MTX-LP2 and SPC-MTX-LP2 formulations were subjected to different kinetic models by using "DDsolver program" (Zhang et al., 2010), i.e., Zero-order, first-order, Higuchi Kinetic, Korsmeyer-Peppas kinetics, and Hixson Crowell, to determine the type of diffusion responsible for the drug release from liposomes (Table 4). Both formulation MTX-LP2 and SPC-MTX-LP2 follow the Korsmeyer-Peppas with an R^2 value of 0.9717 and 0.9761 and release exponent (n) were 0.575 and 0.656, respectively. The Korsmeyer-Peppas model suggested that drug release was driven mainly by a non-Fickian diffusion anomalous transport, and rate of release was a function of t^{n-1}, where n is the release exponent (Costa and Lobo, 2001).

In-vitro cell proliferation studies

The anticancer activity of formulations MTX-LP2 and SPC-MTX-LP2 was performed against human glioblastoma astrocytoma U373-MG cells by using the SRB assay (Skehan et al. 1990; Vichai and Kirtikara 2006). ADR used as a positive control. Fig. 6 showed the activity of formulation against U373-MG cells. The results (Table 5) showed that SPC-MTX-LP2 was significantly more potent than the MTX and MTX-LP2. The GI_{50} were obtained 24.11±0.44 µg/mL and 3.90±0.19 µg/mL MTX-LP2 and SPC-MTX-LP2, respectively.

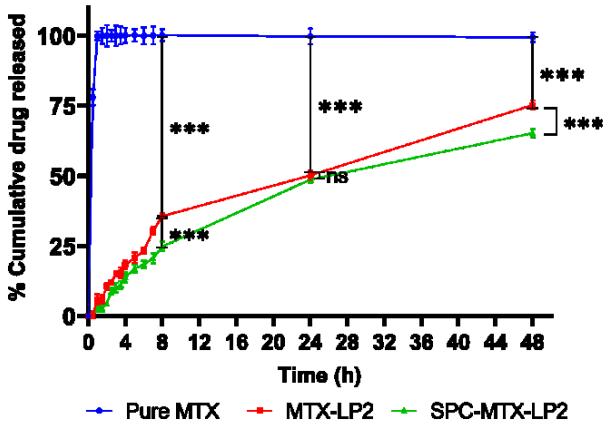

Figure 5. Cumulative percentage drug released by MTX-LP2 and SPC-MTX-LP2 at different interval of times. The comparative releases study for 48 h. in PBS 6.8 pH. The data represented in mean ± SD, n=3 (***$p < 0.001$ and ns > 0.05).

Table 4. The MTX release kinetic models MTX-LP2 and SPC- MTX-LP2 formulations and their respective correlation coefficient

Formulations	The correlation coefficient (R^2)				
	Zero Order	First Order	Higuchi kinetic	Korsmeyer-Peppas	Hixson-Crowell
MTX-LP2	0.7078	0.9292	0.9562	0.9717 n = (0.575)	0.8788
SPC-MTX-LP2	0.8772	0.9668	0.9227	0.9761 n = (0.656)	0.9359

n= estimated from linear regression of log (M_t/M) Vs. log time, where M_t= amount of drug released at time t and M= total amount of drug.

In the present study, we observed that SPC-MTX-LP2 formulation (GI_{50} 3.90±0.19 µg /mL) has promising anticancer activity against U373-MG cells. The GI_{50} of MTX and MTX-LP2 obtained the 23.89±1.82 and 24.11±0.44 µg/mL, respectively. The formulation SPC-MTX-LP2 has significantly more cells inhibition than the plain MTX-LP2. It may occur due to the binding capacity of SPC with PS and PE, which are exposed on the outer membrane of cancer cells. Desai *et al*. (2016) concluded that the significant PS-exposure on the lung cancer cell line (HCC4017) but not in normal bronchial epithelial cells (HBEC30KT). SPC-MTX-LP2 binds with the exposed PS and PE of cancer and MTX was released from the liposomes that increase the membrane fluidity. MTX caused an increase in membrane fluidity described by its interaction with polar phospholipids and fluidized by the hydrophobiccenter of bilayer that causes the alteration of lipids packing and finally causes the membrane disintegration (Pignatello et al., 2005; Maheswari, 2001). Our previous study suggested that SPC-conjugated nanoparticles bind with PS of cancer cells and enhanced cellular uptake via exposed phospholipids caused the more potent anticancer effect than that of non-conjugated nanoparticles and it was also observed that SPC-conjugated nanoparticles found to be safe for the normal cells, which confirms that the SPC is cytotoxic for the cancer cells while safe for the normal healthy cells (Haider et al., 2020). In present research, the cells inhibition capacity of SPC-MTX-LP2 was found to be potent against U373-MG cells, stating that the developed modified formulation would be beneficial for the treatment of cancer.

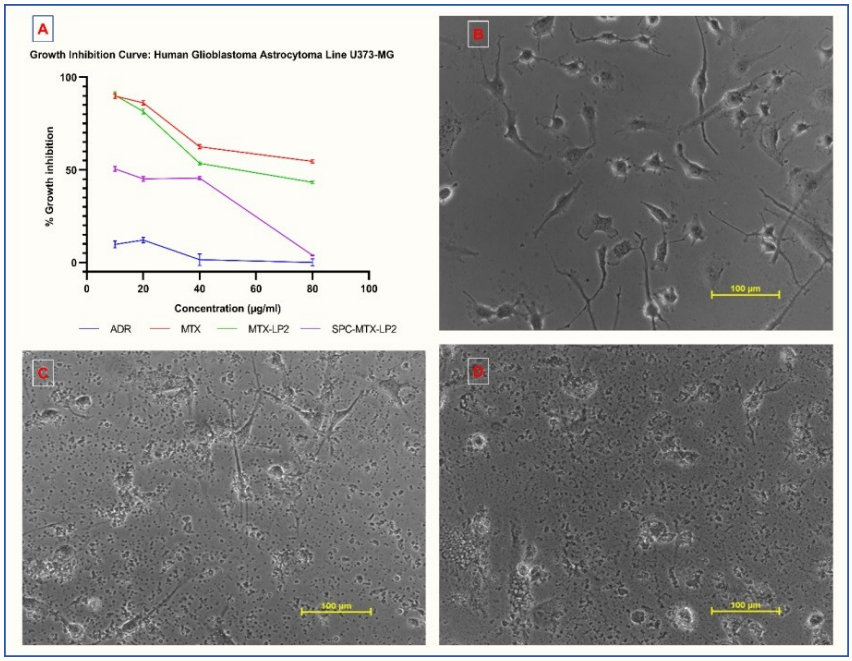

Figure 6. (A) Growth curve: The plot of percentage growth inhibition vs. drug concentration (µg/mL) shows the effective drug concentration on the human glioblastoma astrocytoma cell lineU373-MG cells. Phase-contrast microscopic images of human glioblastoma astrocytoma cell lineU373-MG cells after 24 h. treatment (B) negative control (untreated), (C) MTX-LP2 and (D) SPC-MTX-LP2.

Table 5. Cytotoxic effects of formulations MTX-LP2 and SPC-MTX-LP2 on human glioblastoma astrocytoma cell lineU373-MG cells

Treatment	% Growth Inhibition at concentration (µg/mL)				GI_{50} (µg/mL)
	10	20	40	80	
MTX	89.80±1.27	86.16±1.25	62.46±1.22	54.56±0.90	23.89±1.82
MTX-LP2	90.23±1.84	81.53±1.43	53.47±0.70	43.23±0.66	24.11±0.44
SPC-MTX-LP2	50.50±1.27	45.10±1.21	45.57±0.86	3.90±0.19	3.90±0.19
ADR	9.7±1.88	12.1±1.46	3.2±1.96	0.3±0.51	2.14±0.11

Conclusion

The formulations MTX-LP2 and SPC- MTX-LP2 were successfully prepared by the cast film method. The coating of SPC was done during the rehydration process. The surface morphology of liposomal formulations was spherical, smooth, and vesicle size distribution in the nanometric range. The zeta potential of liposomes was in negative mV, which helps in adherence of formulations with cancer cells and provide maximum cellar uptake. *In vitro* release of MTX from MTX-LP2 and SPC-MTX-LP2 was in a controlled manner with non-Fickian kinetics. *In vitro* cell proliferation study results were suggested that SPC conjugated liposomes showed more potent anticancer activity in the cancer cell line. Such formulations could be further subjected to *in-vitro* cellular uptake, *in-vitro* apoptotic study, western blotting, and *in vivo* antitumor studies to assess their complete therapeutics capabilities.

Ethical statement

This article does not contain any studies with human and animal subjects performed by any of the authors.

Acknowledgements

We thank Sophisticated Instrument Centre of Dr. Harisingh Gour University, Sagar, India for providing the instrumentation facility and Tata Memorial Centre Advanced Centre for Treatment, Research, and Education in Cancer, Mumbai for the *in-vitro* cell proliferation study.

Competing Interests

The authors declare that they have no conflict of interest.

Funding

T. Haider acknowledges the Indian Council of Medical Research (ICMR), New Delhi, for financial support as SRF funding (Grant number for T. Haider 45/7/2018-Nan/BMS).

Authors Contribution

Tanweer Haider and Sandeep Dubey equally contributed in this study. Tanweer Haider conceived and designed the study conception. Sandeep Dubey and Tanweer Haider performed the experiments and analyzed the results. Tanweer Haider, Indu Lata Kanwar and Vikas Pandey prepared the draft manuscript. Vandana Soni supervised, revised and edited of the article. All authors reviewed and approved the final manuscript.

References

Akbarzadeh, A., Rezaei-Sadabady, R., Davaran, S., Joo, S.W., Zarghami, N., Hanifehpour, Y., Samiei, M., Kouhi, M. and K. Nejati-Koshki, (2013). "Liposome: classification, preparation, and applications." *Nanoscale Research Letters,* **8**(1): 102. doi:10.1186/1556-276X-8-102.

Alekseeva, A.A., Moiseeva, E.V., Onishchenko, N.R., Boldyrev, I.A., Singin, A.S., Budko, A.P., Shprakh, Z.S., Molotkovsky, J.G. and E.L. Vodovozova, (2017). "Liposomal formulation of a methotrexate lipophilic prodrug: assessment in tumor cells and mouse T-cell leukemic lymphoma." *International Journal of Nanomedicine,* **12:** 3735-3749. doi:10.2147/IJN.S133034.

Alves, A. C., Ribeiro, D., Nunes, C. and S. Reis, (2016). "Biophysics in cancer: The relevance of drug-membrane interaction studies." *Biochim Biophys Acta Biomembr,* **1858**(9): 2231-2244. doi:10.1016/j.bbamem.2016.06.025.

Costa, P. and J. M. S. Lobo, (2001). "Modeling and comparison of dissolution profiles." *European Journal of Pharmaceutical Sciences,* **13**(2): 123-133. doi:10.1016/s0928-0987(01)00095-1.

Desai, T. J., Toombs, J. E., Minna, J. D., Brekken, R. A. and D. G. Udugamasooriya, (2016). "Identification of lipid-phosphatidylserine (PS) as the target of unbiasedly selected cancer specific peptide-peptoid hybrid PPS1." *Oncotarget,* **7**(21): 30678-30690. doi:10.18632/oncotarget.8929.

Dubey, P. K., Mishra, V., Jain, S., Mahor, S. and S. P. Vyas, (2004). "Liposomes modified with cyclic RGD peptide for tumor targeting." *Journal of Drug Targeting,* **12**(5): 257-264. doi:10.1080/10611860410001728040.

Ejikeme, P. C. N., Ejikeme, M. E. and B. N. Abalu, (2013). "RSM optimization process for uptake of water from ethanol water solution using oxidized starch." *The Pacific Journal of Science and Technology*, **14:** 319-329.

Elvas, F., Stroobants, S. and L. Wyffels, (2017). "Phosphatidylethanolamine targeting for cell death imaging in early treatment response evaluation and disease diagnosis." *Apoptosis,* **22**(8): 971-987. doi:10.1007/s10495-017-1384-0.

Emoto, K., Toyama-Sorimachi, N., Karasuyama, H., Inoue, K. and M. Umeda, (1997). "Exposure of phosphatidylethanolamine on the surface of apoptotic cells." *Experimental Cell Research,* **232**(2): 430-434. doi:10.1006/excr.1997.3521.

Fadok, V. A., Voelker, D. R., Campbell, P. A., Cohen, J. J., Bratton, D. L. and P. M. Henson, (1992). "Exposure of phosphatidylserine on the surface of apoptotic lymphocytes triggers specific recognition and removal by macrophages." *Journal of Immunology,* **148**(7): 2207-2216. doi:10.1007/s13238-010-0076-0.

Ferreira, S. L., Bruns R. E., Ferreira, H. S., Matos, G. D., David, J. M., Brandão, G. C., da Silva, E. G., Portugal, L. A., dos Reis, P. S., Souza, A. S. and W. N. dos Santos, (2007). "Box-Behnken design: an alternative for the optimization of analytical methods." *Analytica Chimica Acta*, **597**(2): 179-86. doi: 10.1016/j.aca.2007.07.011.

Fry, D. W., White, J. C. and I. D. Goldman, (1979). "Alterations of the carrier-mediated transport of an anionic solute, methotrexate, by charged liposomes in Ehrlich ascites tumor cells." *Journal of Membrane Biology*, **50**(2): 123-140. doi:10.1007/bf01868944.

García-Beleño, J. and E. Rodríguez de San Miguel, (2021). "Integration of Response Surface Methodology (RSM) and Principal Component Analysis (PCA) as an optimization tool for polymer inclusion membrane based-optodes designed for Hg(II), Cd(II), and Pb(II)." *Membranes*, **11:** 288. doi: 10.3390/membranes11040288.

Gottschalk, O., Metz, P., Dao Trong, M. L., Altenberger, S., Jansson, V., Mutschler, W. and M. Schmitt-Sody, (2015). "Therapeutic effect of methotrexate encapsulated in cationic liposomes (EndoMTX) in comparison to free methotrexate in an antigen-induced arthritis study *in vivo*." *Scandinavian Journal of Rheumatology,* **44**(6): 456-463. doi:10.3109/03009742.2015.1030448.

Grzybek, M., Chorzalska, A., Bok, E., Hryniewicz-Jankowska, A., Czogalla, A., Diakowski, W. and A. F. Sikorski, (2006). "Spectrin–phospholipid interactions: Existence of multiple kinds of binding sites?" *Chemistry and Physics of Lipids,* **141**(1-2): 133-141. doi:10.1016/j.chemphyslip.2006.02.008.

Gutschner, T. and S. Diederichs, (2012). "The hallmarks of cancer: a long non-coding RNA point of view." *RNA Biology,* **9**(6): 703-719. doi:10.4161/rna.20481.

Haider, T., Pandey, V., Behera, C., Kumar, P., Gupta, P. N. and V. Soni, (2020). "Spectrin conjugated PLGA nanoparticles for potential membrane phospholipid interactions: Development, optimization and *in vitro* studies." *Journal of Drug Delivery Science and Technology,* **60**: 102087. doi:10.1016/j.jddst.2020.102087.

Haider, T., Tiwari, R., Vyas, S. P. and V. Soni, (2019). "Molecular determinants as therapeutic targets in cancer chemotherapy: An update." *Pharmacology & Therapeutics,* **200:** 85-109. doi:10.1016/j.pharmthera.2019.04.011

Jain, S. K., Haider, T., Kumar, A. and A. Jain, (2016). "Lectin-conjugated clarithromycin and acetohydroxamic acid-loaded plga nanoparticles: a novel approach for effective treatment of H pylori." *AAPS PharmSciTech,* **17**(5): 1131-1140. doi:10.1208/s12249-015-0443-5.

Jin, S., DiPaola, R. S., Mathew, R. and E. White, (2007). "Metabolic catastrophe as a means to cancer cell death." *Journal of Cell Science,* **120**(3): 379-383. doi:10.1242/jcs.03349.

Joseph, E. and G. Singhvi, (2019). "Multifunctional nanocrystals for cancer therapy: a potential nanocarrier." In: A. M. Grumezescu (Ed.), *Nanomaterials for Drug Delivery and Therapy*, William Andrew Publishing, pp. 91-116.

Korgel, B. A., van Zanten, J. H. and H. G. Monbouquette, (1998). "Vesicle size distributions measured by flow field-flow fractionation coupled with multiangle light scattering." *Biophysical Journal,* **74**(6): 3264-3272. doi:10.1016/S0006-3495(98)78033-6.

Lakkadwala, S., dos Santos Rodrigues, B., Sun, C. and J. Singh, (2019). "Dual functionalized liposomes for efficient co-delivery of anti-cancer chemotherapeutics for the treatment of glioblastoma." *Journal of Controlled Release,* **307**: 247-260. doi:https://doi.org/10.1016/j.jconrel.2019.06.033.

Lujan, H., Griffin, W. C., Taube, J. H. and C. M. Sayes, (2019). "Synthesis and characterization of nanometer-sized liposomes for encapsulation and microRNA transfer to breast cancer cells." *International Journal of Nanomedicine,* **14**: 5159-5173. doi:10.2147/IJN.S203330.

Machnicka, B., Grochowalska, R., Boguslawska, D. M., Sikorski, A. F. and M. C. Lecomte, (2012). "Spectrin-based skeleton as an actor in cell signaling." *Cellular and Molecular Life Sciences,* **69**(2): 191-201. doi:10.1007/s00018-011-0804-5.

Maheswari, K. U. (2001). "Lipid bilayer–methotrexate interactions: A basis for methotrexate neurotoxicity." *Current Science,* **81**(4): 571-574.

Malam, Y., Loizidou, M. and A. M. Seifalian, (2009). "Liposomes and nanoparticles: nanosized vehicles for drug delivery in cancer." *Trends in Pharmacological Sciences,* **30**(11): 592-599. doi:https://doi.org/10.1016/j.tips.2009.08.004.

Manojlovic, V., Winkler, K., Bunjes, V., Neub, A., Schubert, R., Bugarski, B. and G. Leneweit, (2008). "Membrane interactions of ternary phospholipid/cholesterol bilayers and encapsulation efficiencies of a RIP II protein." *Colloids and Surfaces B: Biointerfaces,* **64**(2): 284-296. doi:10.1016/j.colsurfb.2008.02.001.

Myers, R.H., Montgomery, D.C. and C.M. Anderson-Cook, (2016). "Response surface methodology: process and product optimization using designed experiments." John Wiley & Sons "New York, NY, USA, p. 856; ISBN 978-1-118-91601-8.

Mizuguchi, M., Nara, M., Kawano, K. and K. Nitta, (1997). "FT-IR study of the Ca^{2+}- binding to bovine α- lactalbumin: Relationships between the type of coordination and characteristics of the bands due to the Asp COO− groups in the Ca^{2+}- binding site." *FEBS Letters,* **417**(1): 153-156. doi:10.1016/S0014-5793(97)01274-X.

Mombers, C., de Gier, J., Demel, R. A. and L. L. van Deenen, (1980). "Spectrin-phospholipid interaction: A monolayer study." *Biochimica et Biophysica Acta,* **603**(1): 52-62. doi:10.1016/0005-2736(80)90390-9.

Mozafari, M. (2010). "Nanoliposomes: preparation and analysis." (In V. Weissig (Ed.), *Liposomes. Methods in Molecular Biology (Methods and Protocols),* Humana Press. **605:** pp. 29-50.

Nara, M., Tasumi, M., Tanokura, M., Hiraoki, T., Yazawa, M. and A. Tsutsumi, (1994). "Infrared studies of interaction between metal ions and Ca2+-binding proteins Marker bands for identifying the types of coordination of the side-chain COO− groups to metal ions in pike parvalbumin (pI= 4.10)." *FEBS Letters,* **349**(1): 84-88. doi:10.1016/0014-5793(94)00645-8.

Neves, L. F. F., Krais, J. J., Van Rite, B. D., Ramesh, R., Resasco, D. E. and R. G. Harrison, (2013). "Targeting single-walled carbon nanotubes for the treatment of breast cancer using photothermal therapy." *Nanotechnology,* **24**(37): 375104. doi:10.1088/0957-4484/24/37/375104.

Ong, S. G., Ming, L. C., Lee, K. S. and K. H. Yuen, (2016). "Influence of the encapsulation efficiency and size of liposome on the oral bioavailability of griseofulvin-loaded liposomes." *Pharmaceutics,* **8**(3): 25. doi:10.3390/pharmaceutics8030025.

Pandey, A. N., Raj, R., Ganesh, N. and S. K. Jain, (2018). "Concanavalin-A conjugated 5-fluorouracil loaded PLGA nanoparticles: A novel approach for effective treatment of colorectal cancer." *Research Journal of Pharmacy and Technology,* **11**(7): 2782-2791. doi:10.5958/0974-360x.2018.00514.0.

Patel, K., Doddapaneni, R., Sekar, V., Chowdhury, N., and M. Singh, (2016). "Combination approach of YSA peptide anchored docetaxel stealth liposomes with oral antifibrotic agent for the treatment of lung cancer." *Molecular Pharmaceutics,* **13**(6): 2049-2058. doi:10.1021/acs.molpharmaceut.6b00187.

Pathak, D. and R. Mallik, (2017). "Lipid - motor interactions: Soap opera or symphony?" *Current Opinion in Cell Biology,* **44**: 79-85. doi:10.1016/j.ceb.2016.09.005.

Patra, J.K., Das, G., Fraceto, L.F., Campos, E.V.R., del Pilar Rodriguez-Torres, M., Acosta-Torres, L.S., Diaz-Torres, L.A., Grillo, R., Swamy, M.K., Sharma, S. and S. Habtemariam, (2018). "Nano based drug delivery systems: recent developments and future prospects." *Journal of Nanobiotechnology,* **16**(1): 71. doi:10.1186/s12951-018-0392-8.

Pignatello, R., Di Guardo, L., Puleo, A. and G. Puglisi, (2005). "Lipophilic conjugates of methotrexate with glucosyl-lipoamino acids: calorimetric study of the interaction with a biomembrane model." *Thermochimica Acta,* **426**(1-2): 163-171. doi:10.1016/j.tca.2004.07.017.

Quinn, P. J. (2004). "Plasma membrane phospholipid asymmetry." In: Quinn, P. J. and V. E. Kagan, (Eds.), *Phospholipid Metabolism in Apoptosis,* Springer, Boston, MA. **36:** 39-60.

Ray, S. and A. Chakrabarti, (2004). "Membrane interaction of erythroid spectrin: surface-density-dependent high-affinity binding to phosphatidylethanolamine." *Molecular Membrane Biology,* **21**(2): 93-100. doi:10.1080/09687680310001625800.

Robinson, T.J. (2014). *Box-Behnken Designs*. In Wiley StatsRef: Statistics Reference Online (Eds: N. Balakrishnan, T. Colton, B. Everitt, W. Piegorsch, F. Ruggeri and J.L. Teugels). doi:10.1002/9781118445112.stat04101.

Sharma, B. and S.S. Kanwar, (2018). "Phosphatidylserine: A cancer cell targeting biomarker." *Seminars in Cancer Biology,* **52**(Pt 1): 17-25. doi:10.1016/j.semcancer.2017.08.012.

Sikorski, A. F., Hanus-Lorenz, B., Jezierski, A. and A. R. Dluzewski, (2000). "Interaction of membrane skeletal proteins with membrane lipid domain." *Acta Biochimica Polonica,* **47**(3): 565-578.

Silva, R., Ferreira, H., Little, C. and A. Cavaco-Paulo, (2010). "Effect of ultrasound parameters for unilamellar liposome preparation." *Ultrasonics Sonochemistry,* **17**(3): 628-632. doi:10.1016/j.ultsonch.2009.10.010.

Skehan, P., Storeng, R., Scudiero, D., Monks, A., McMahon, J., Vistica, D., Warren, J.T., Bokesch, H., Kenney, S. and M.R. Boyd, (1990). "New colorimetric cytotoxicity assay for anticancer-drug screening." *Journal of the National Cancer Institute,* **82**(13): 1107-1112. doi:10.1093/jnci/82.13.1107.

Soni, V., Kohli, D. V. and S. K. Jain, (2007). "Transferrin coupled liposomes for enhanced brain delivery of doxorubicin." *Vascular Disease Prevention,* **4**(1): 31-38. doi:10.2174/1567270010704010031.

Soni, V., Kohli, D. V. and S. K. Jain, (2008). "Transferrin-conjugated liposomal system for improved delivery of 5-fluorouracil to brain." *Journal of Drug Targeting,* **16**(1): 73-78. doi:10.1080/10611860701725381.

Sou, K. (2011). "Electrostatics of carboxylated anionic vesicles for improving entrapment capacity." *Chemistry and Physics of Lipids,* **164**(3): 211-215. doi:10.1016/j.chemphyslip.2011.01.002.

Spector, A. A. and M. A. Yorek, (1985). "Membrane lipid composition and cellular function." *Journal of Lipid Research,* **26**(9): 1015-1035.

Sugimura, M., Donato, R., Kakkar, V. V. and M. F. Scully, (1994). "Annexin-V as a probe of the contribution of anionic phospholipids to the procoagulant activity of tumor-cell surfaces." *Blood Coagulation and Fibrinolysis,* **5**(3): 365-373.

Tiwari, R., Viswanathan, K., Vyas, S. P. and V. Soni, (2020). "*In vitro* evaluation of lectinized cisplatin bearing liposomes system." *International Journal of Applied Pharmaceutics*, **7**: 60-64. doi:10.22159/ijap.2020v12i6.39350.

Vichai, V. and K. Kirtikara, (2006). "Sulforhodamine B colorimetric assay for cytotoxicity screening." *Nature Protocols,* **1**(3): 1112-1116. doi:10.1038/nprot.2006.179.

Wang, L., Zhang, M., Zhang, N., Shi, J., Zhang, H., Li, M., Lu, C. and Z. Zhang, (2011). "Synergistic enhancement of cancer therapy using a combination of docetaxel and photothermal ablation induced by single-walled carbon nanotubes." *International Journal of Nanomedicine,* **6:** 2641-2652. doi:10.2147/IJN.S24167.

Winter, P. M., Pearce, J., Chu, Z., McPherson, C. M., Takigiku, R., Lee, J. H. and X. Qi, (2015). "Imaging of brain tumors with paramagnetic vesicles targeted to phosphatidylserine." *Journal of Magnetic Resonance Imaging,* **41**(4): 1079-1087. doi:10.1002/jmri.24654.

Woodbury, D. J., Richardson, E. S., Grigg, A. W., Welling, R. D. and B. H. Knudson, (2006). "Reducing liposome size with ultrasound: bimodal size distributions." *Journal of Liposome Research,* **16**(1): 57-80. doi:10.1080/08982100500528842.

World Health Organisation, WHO (2021). "Cancer." *Fact sheets.* Retrieved from https://www.who.int/news-room/fact-sheets/detail/cancer [21 September 2021].

Zhang, Y., Huo, M., Zhou, J., Zou, A., Li, W., Yao, C. and S. Xie, (2010). "DDSolver: an add-in program for modeling and comparison of drug dissolution profiles." *The AAPS journal,* **12**(3): 263-271. doi:10.1208/s12248-010-9185-1.

Zhang, Y., Yang, M., Portney, N.G., Cui, D., Budak, G., Ozbay, E., Ozkan, M. and C.S. Ozkan, (2008). "Zeta potential: a surface electrical characteristic to probe the interaction of nanoparticles with normal and cancer human breast epithelial cells." *Biomedical Microdevices,* **10**(2): 321-328. doi:10.1007/s10544-007-9139-2.

Zwaal, R. F. and A. J. Schroit, (1997). "Pathophysiologic implications of membrane phospholipid asymmetry in blood cells." *Blood,* **89**(4): 1121-1132. doi:10.1182/blood.V89.4.1121.

